nature climate change

LETTERS

PUBLISHED ONLINE: 17 NOVEMBER 2013 | DOI: 10.1038/NCLIMATE2051

Robust spatially aggregated projections of climate extremes

E. M. Fischer*, U. Beyerle and R. Knutti

Many climatic extremes are changing[1–5], and decision-makers express a strong need for reliable information on further changes over the coming decades as a basis for adaptation strategies. Here, we demonstrate that for extremes stakeholders will have to deal with large irreducible uncertainties on local to regional scales as a result of internal variability, even if climate models improve rapidly. A multimember initial condition ensemble carried out with an Earth system model shows that trends towards more intense hot and less intense cold extremes may be masked or even reversed locally for the coming three to five decades even if greenhouse gas emissions rapidly increase. Likewise, despite a long-term trend towards more intense precipitation and longer dry spells, multidecadal trends of opposite sign cannot be excluded over many land points. However, extremes may dramatically change at a rate much larger than anticipated from the long-term signal. Despite these large irreducible uncertainties on the local scale, projections are remarkably consistent from an aggregated spatial probability perspective. Models agree that within only three decades about half of the land fraction will see significantly more intense hot extremes. We show that even in the short term the land fraction experiencing more intense precipitation events is larger than expected from internal variability. The proposed perspective yields valuable information for decision-makers and stakeholders at the international level.

Significant changes to more hot and less cold extremes and record events have been observed over several regions[1–3] and identified in globally aggregated approaches[4,5]. Attribution studies argue that anthropogenic influence has enhanced the probability of the occurrence of some types of temperature and precipitation extremes occurring[6–11]. Recent projections suggest that these trends continue along with rising anthropogenic greenhouse gas emissions[12–16]. Model simulations from the Coupled Model Intercomparison Project Phase 5 (CMIP5) project pronounced warming of the annual temperature maxima (TXx, hereafter referred to as hot extremes, see Methods) and minima (TNn, cold extremes) as well as widespread changes in maximum five-day accumulated precipitation (RX5day, heavy precipitation intensity) and annual maxima of consecutive number of dry days (CDD, dry spell length)[17]. The changes by mid-century (2041–2060) shown in Fig. 1 (left) based on an extended set of 25 CMIP5 models (see Supplementary Information) are largely consistent with those projected for the end of the twenty-first century in refs 12,13. Projections for all four extreme indices are associated with very large uncertainties[12]. At many grid points individual models simulate warming of hot and cold extremes that is almost twice the multimodel mean (Supplementary Fig. 1, right) and others show hardly any change or even a slight cooling at some grid points despite the strong global warming in the Representative Concentration Pathway 8.5 (RCP8.5) scenario (Supplementary Fig. 1, left). Uncertainties are even larger for precipitation extremes. Despite a general tendency towards heavier precipitation intensity and longer dry spells, opposite trends are found at most grid points by 2041–2060 in at least two models (Supplementary Fig. 1).

Do these uncertainties point to major model deficiencies that prevent us from making any reliable projections in climate extremes? Not necessarily. We show here that the uncertainties largely result from internal climate variability and would remain even in a perfect model. To quantify the role of internal variability that is unpredictable owing to initial condition uncertainties, we run the Community Earth System Model (CESM) 21 times from 1950–2100 with slightly differing atmospheric initial conditions (hereafter referred to as CESM-IC) but otherwise identical model configuration and forcing (historical and RCP8.5; see Methods; Supplementary Figs 2 and 3). The CESM-IC multimember mean (Fig. 1, right) shows changes remarkably similar to the CMIP5 multimodel mean (Fig. 1, left). Even using one single model the low estimates (5th percentile, second lowest member) and high estimate (95th percentile, second highest member) for the 20-year mean changes in cold and hot extremes by the mid-century locally vary from $-1\,^{\circ}C$ to $+7\,^{\circ}C$ for cold and $+1.5\,^{\circ}C$ to $5.5\,^{\circ}C$ for hot extremes, respectively (Supplementary Fig. 4). Likewise, different members do not agree on the sign of changes in dry spell length and heavy precipitation intensity.

We refer to the multimember mean across CESM-IC (Fig. 1, right), as an estimate of the forced signal, that is, the response to the imposed forcing in the absence of variability. The departures from this forced signal arise from internal variability inherent to the coupled climate system (for example, modes of variability such as the El Niño–Southern Oscillation, Madden–Julian Oscillation or short-term synoptic variability)[18]. Daily extremes are particularly sensitive to variability on decadal, interannual to subseasonal timescales[19,20]. CESM-IC samples only this internal variability, whereas CMIP5 additionally samples parametric and structural model uncertainties. By mid-century the uncertainty range induced by internal variability (here expressed as 2σ across CESM-IC locally) corresponds on average to roughly 40% of the CMIP5 uncertainty for hot and 60% for cold extremes, and more than 75% for heavy precipitation intensity and dry spell length (Supplementary Fig. 5). About 10 years after the initial perturbation, the timescale of decadal predictability, the multimember range across CESM-IC no longer increases in time (Supplementary Fig. 3) and covers roughly the same uncertainty range as an eleven-member CESM ensemble initialized from different starting points in the control simulations (different ocean initial conditions, not shown). The uncertainties in CESM-IC need to be interpreted with caution as they are based

Institute for Atmospheric and Climate Science, ETH Zurich, Universitätstrasse 16, 8092 Zurich, Switzerland. *e-mail: erich.fischer@env.ethz.ch

© 2013 Macmillan Publishers Limited. All rights reserved.

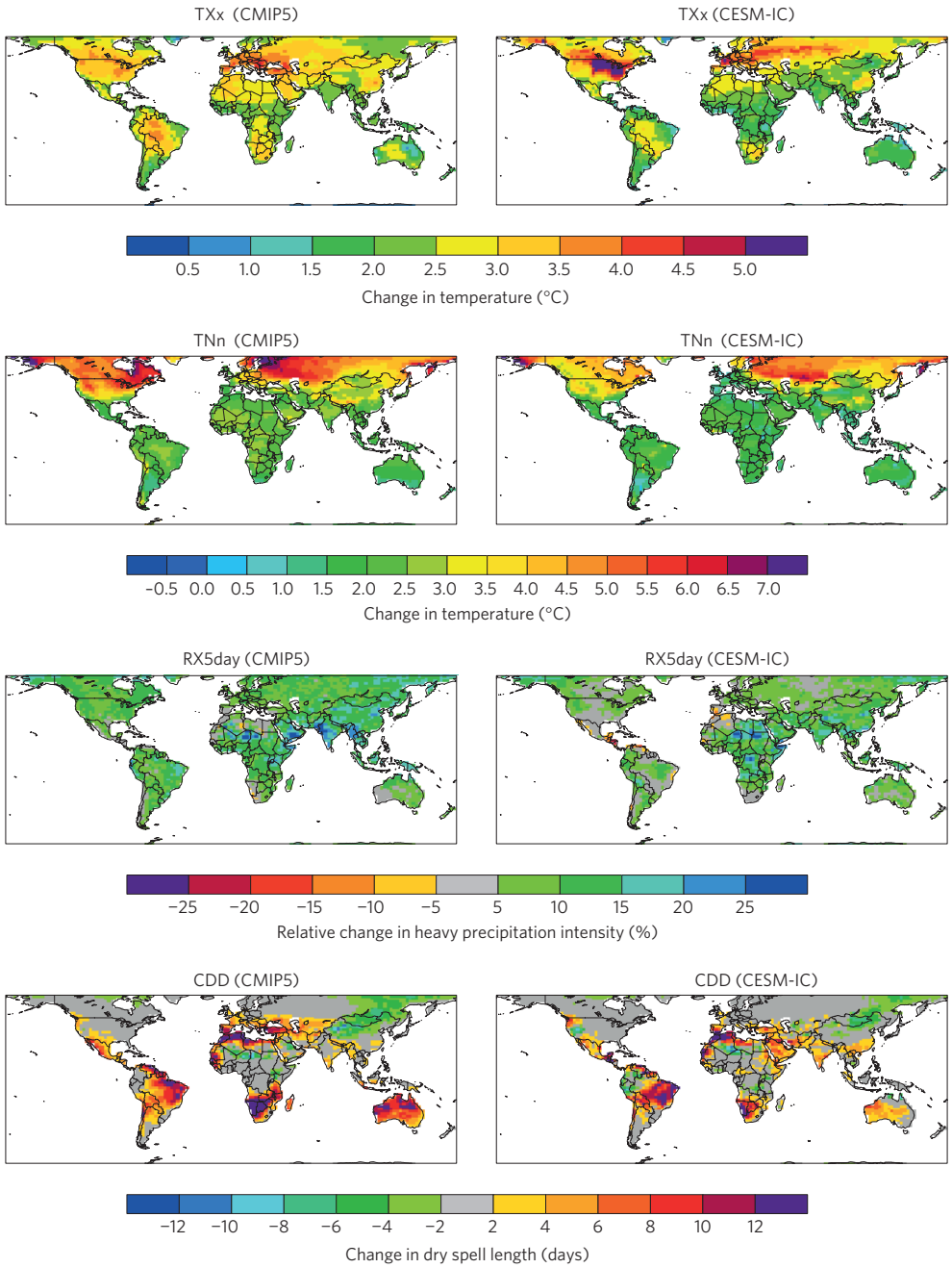

Figure 1 | Changes in extremes by the mid-twenty-first century. Projected changes in intensity of hot extremes (TXx, first row) and cold extremes (TNn, second row), heavy precipitation intensity (RX5day, third row) and dry spell length (CDD, last row) in 2041–2060 with respect to 1986–2005 for the RCP8.5 scenario. The left panels show the multimodel mean average changes across 25 CMIP5 models and the right panels the multimember average across 21 CESM-IC members.

on the assumption that CESM reliably represents the internal variability in extreme indices. The assumption that the estimate is reasonable is supported by the fact that the uncertainties across CESM-IC are consistent with a ten-member initial condition ensemble for the Commonwealth Scientific and Industrial Research Organisation model (CSIRO-Mk3-6-0; Supplementary Fig. 5), the largest ensemble available in the CMIP5 archive, and the fact that the simulated interannual variability, the dominant contribution to internal variability, in the extremes indices is in reasonable agreement with the ERA Interim and NCEP-DOE-2 reanalyses as well as the gridded observational HadEX2 and GHCNDEX data sets. Except for the interannual variability in heavy precipitation intensity over the tropics, which is biased low, the variability in the reanalyses for the period 1986–2005 falls within the range of variability realizations of the CESM-IC members (see Supplementary Figs 6 and 7 and evaluation section in Supplementary Information).

The role of uncertainty induced by internal variability has been shown to be dominant for decadal and seasonal mean changes in the next decades[21,22]. We here argue that for changes in extremes it is the dominant uncertainty source even for several decades. The role of internal variability generally decreases if mean temperatures or extreme indices are averaged across regions[23] or the globe. For instance, all the CESM-IC members show very similar global temperature increases by the end of the twenty-first century (Supplementary Fig. 2). However, large

© 2013 Macmillan Publishers Limited. All rights reserved.

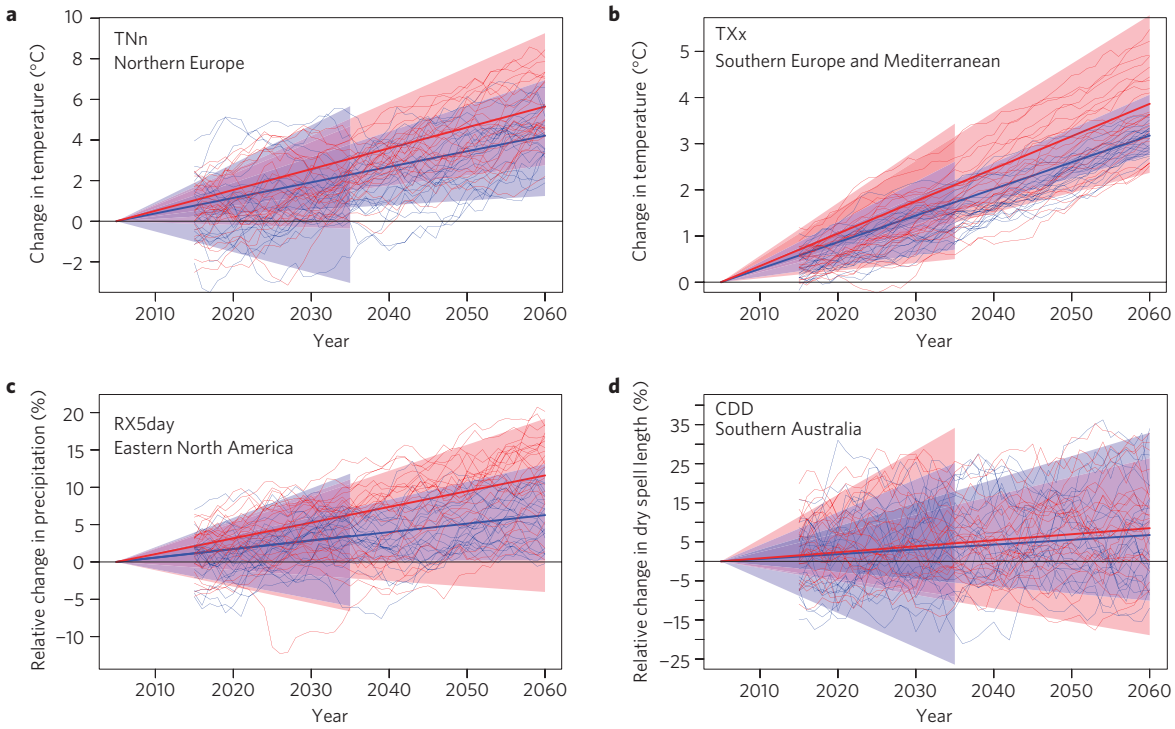

Figure 2 | Uncertainties in projected trends of extremes. a–d, Range of lowest to highest regional linear trends in CESM-IC (blue cones) and CMIP5 (red cones) for the periods 2005–2035 and 2005–2060. For illustrative purposes the linear trends are adjusted so that they all start with the same value in 2005. The thick lines mark the CMIP5 multimodel mean (thick red lines) and CESM-IC multimember mean trend (thick blue lines). The 11-year running means of the annual indices are shown for each CMIP5 model (red) and each CESM-IC member (blue). Projected trends are averaged for TNn across land grid points in Northern Europe (**a**, 48–75° N, 10° W–40° E), for TXx averaged over Southern Europe and the Mediterranean (**b**, 30–48° N, 10° W–40° E), for RX5day averaged over eastern North America (**c**, 25–50° N, 50–85° W) and for CDD averaged over Southern Australia (**d**, 30–45° S, 110–155° E).

uncertainties in temperature and precipitation extremes remain even if multidecadal trends are averaged across large regions, as shown here in illustrative examples (Fig. 2). Averaged across northern Europe individual members show warming trends in the cold extremes of $<1\,^{\circ}C$ to $>6\,^{\circ}C$ for the period 2005–2060. Likewise, some members show no trend in heavy rainfall intensity until 2060 over eastern North America, whereas others project an increase at twice the rate of the mean long-term forced signal. This divergence of linear trends induced by internal variability is even more pronounced for trends from 2005–2035. On the century timescale (2005–2100) regional trends are more robust. We also expect a lower sensitivity to internal variability in extreme indices quantifying the exceedance frequency of moderate thresholds that mainly follow the mean changes such as TN90 or tropical nights[12,17]. However, if the forced signal is small or the variability large as for dry spell length in Southern Australia (Fig. 2d), we would not expect models or CESM-IC members to agree on the sign even by the end of the twenty-first century[24,25].

Our findings underline that it will not be possible to provide the information on local changes in extremes that would be desirable for local stakeholders. The uncertainty owing to internal variability is dominant and is essentially irreducible, as there is no atmospheric predictability on multidecadal timescales, while the model uncertainty can potentially be reduced. For a robust assessment of the forced model signal in extremes, which will ultimately dominate the response on longer timescales, it is necessary to carry out large initial condition ensembles as in ref. 26. However, it would be dangerous to design a strategy to adapt solely to a well-constrained forced signal. Instead, adaptation and planning should take into account the range of possible outcomes, which could ideally be derived from a large multimember ensemble carried out with numerous models.

Does the lack of clear local trends preclude robust statements about changes in extremes? Such an interpretation would be clearly misleading. No simulation shows a pattern of quasi-uniform reduction in heavy precipitation as in Supplementary Fig. 4, or any of the other lowest or highest estimates at every grid point. The internal variability rather induces an uncertainty on where changes occur in different members. To illustrate this effect we calculate a spatial probability density function (PDF) across the 20-year mean changes at all land grid points between 66° S and 66° N (Fig. 3). For the cold and hot extremes the 20-year mean changes are normalized by the local σ across annual values of the extreme index in the control period 1986–2005. The PDFs illustrate the land fraction in CMIP5 models (red lines) or CESM-IC members (blue lines) experiencing a certain change.

There is remarkable agreement among all CESM-IC members that significant changes in temperature extremes occur in the next decades. Already by 2016–2035 about 27–46% of the land area experiences changes in hot extremes larger than 1σ and 16–30% for cold extremes. Note that even in control simulations representing an undisturbed climate state there would be local differences in 20-year means of extreme indices at most grid points. The distribution of these local differences is estimated from grid point differences between all possible pairs of the 21 members in the control period 1986–2005 (grey). The projected changes already exceed those expected in an undisturbed climate by 2016–2035. There is high agreement across CESM-IC members that within only three decades (by 2016–2035 relative to 1986–2005) about 60–70% of the land fraction will experience significant changes in hot and 42%–55% in cold extremes (Supplementary Fig. 8). The remarkable agreement across CESM-IC illustrates that, despite large local uncertainties induced by internal variability, the area exhibiting certain changes is similar in each realization. As the

© 2013 Macmillan Publishers Limited. All rights reserved.

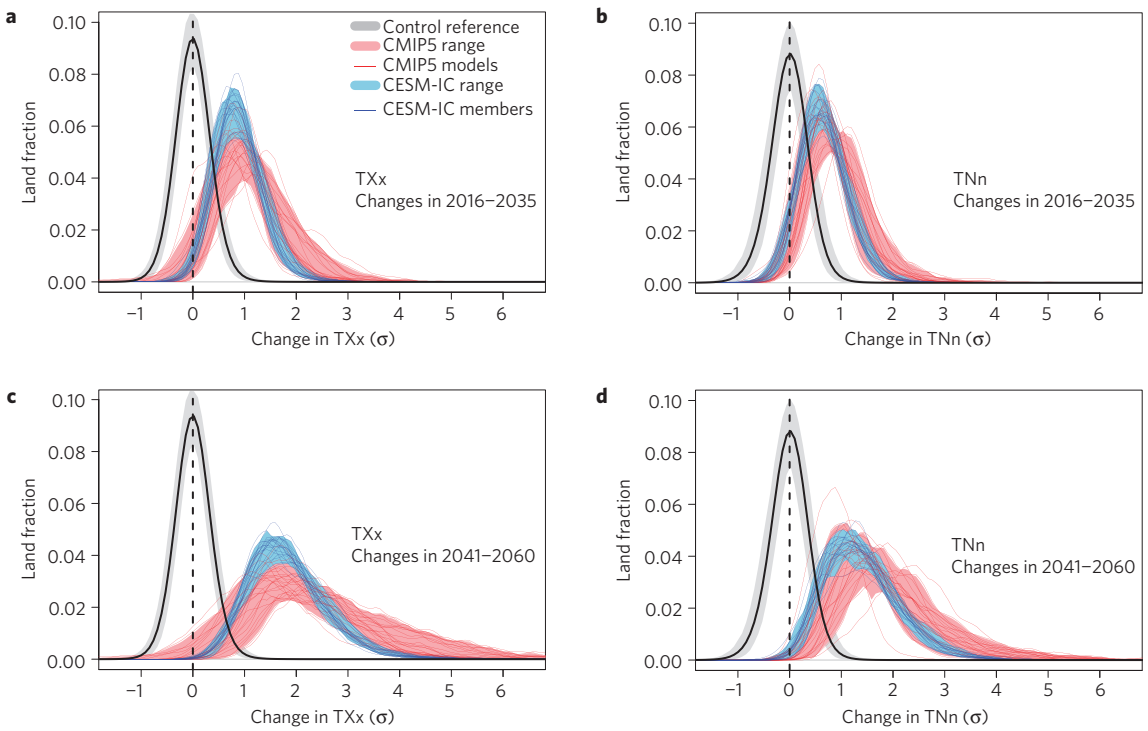

Figure 3 | Spatial distribution of changes in hot and cold extremes. a–d, PDF of the land fraction (66° S–66° N) experiencing a certain 20-year mean change in hot (**a**,**c**) and cold (**b**,**d**) extremes. 20-year mean changes are shown for the period 2016–2035 (**a**,**b**) and 2041–2060 (**c**,**d**) with respect to the 20-year mean in 1986–2005. Legend in **a** applies to all panels. The red lines mark individual models of CMIP5 and red shading the 5th to 95th percentile across the models for each bin marking a certain change. Likewise the blue lines show the individual CESM-IC members and the blue shading the respective range across different members. The changes expected owing to internal variability are shown as grey shading with the solid black line marking the mean. Twenty-year mean changes at each grid point are normalized by the interannual standard deviation of the respective annual extreme index values for 1986–2005. See Supplementary Fig. 10 for the corresponding figure with absolute temperature changes.

changes increase by the mid-twenty-first century, members still agree on what fraction of the land experiences changes larger than a given threshold. Also the CMIP5 models (red range) show reasonably consistent changes in the spatial PDFs of temperature extremes (Fig. 3). The differences between CMIP5 models largely arise from their different transient global temperature response. If corrected for, they also show a remarkably robust spatial PDF, for example, for a 2 °C warming (Supplementary Fig. 9). Figure 3 does not show the absolute temperature changes, but even these are reasonably consistent (Supplementary Fig. 10). Note that many CMIP5 models have substantially heavier upper tails than CESM members and the uncertainties across CMIP5 are particularly large in the tail, which implies that model uncertainties are dominant for the maximum warming.

Even for heavy precipitation intensity there is high agreement across CESM-IC members and reasonable agreement across CMIP5 models on the land fractions experiencing certain changes (Fig. 4). Already by 2016–2035 all CESM-IC members consistently project more than 10% increase in heavy precipitation intensity at a land fraction of 20–30%. Likewise, all CMIP5 models except INM-CM4 simulate substantial changes in the near future. For dry spell length most models show only a weak signal and do not agree whether most of the land fraction experiences longer or shorter dry spells. However, in many models the PDF widens, implying that a larger area than expected by internal variability experiences longer dry spells by the mid-century (Fig. 4). For all indices CESM-IC members show good agreement, which suggests a potential to narrow down the uncertainty in this spatial perspective with further model development as the spatial PDFs are hardly sensitive to internal variability.

To provide an analogy, it is impossible to predict the time and location of the next traffic accident in a city. But there will be one somewhere, so it makes sense to have an ambulance ready. Higher speed limits will result in more accidents and will require more ambulances, even if it remains impossible to predict the locations of future accidents. Thereby some aggregated aspects are predictable even if the single events are not. Our findings show that with a global spatial probability perspective robust projections for extremes are possible even for the near future. The perspective is more informative than a global mean and when taking into account local vulnerabilities it may be promising in many fields, such as the reinsurance business with globally distributed portfolios, the global commodity market or strategies for global food security.

The models used here do not resolve small-scale heavy precipitation events and have deficiencies in representing dynamical features such as the blocking frequency and persistence driving temperature extremes in mid-latitudes[27]. Moreover, the estimates for interannual variability in precipitation extremes and therefore the associated uncertainty are found to be rather low. Thus, we see value in further refining and developing models even though uncertainties in regional projection of extremes will remain substantial.

Our findings imply that the traditional evaluation of the projection agreement at the grid-point level has weaknesses. Models disagree on the exact location of changes in precipitation owing to differences in their present-day climatology[28,29] and internal variability[23–25]. But the perception that models allow no robust statements about changes in the magnitude of extremes in the near future is misleading. We demonstrate that from a spatial probability perspective, they provide remarkably robust evidence for more intense hot and less intense cold extremes, and heavier precipitation already on timescales of two or three decades. These are robust even for single continents or large countries. For example, hot extremes are projected to increase strongly in a large fraction of

© 2013 Macmillan Publishers Limited. All rights reserved.

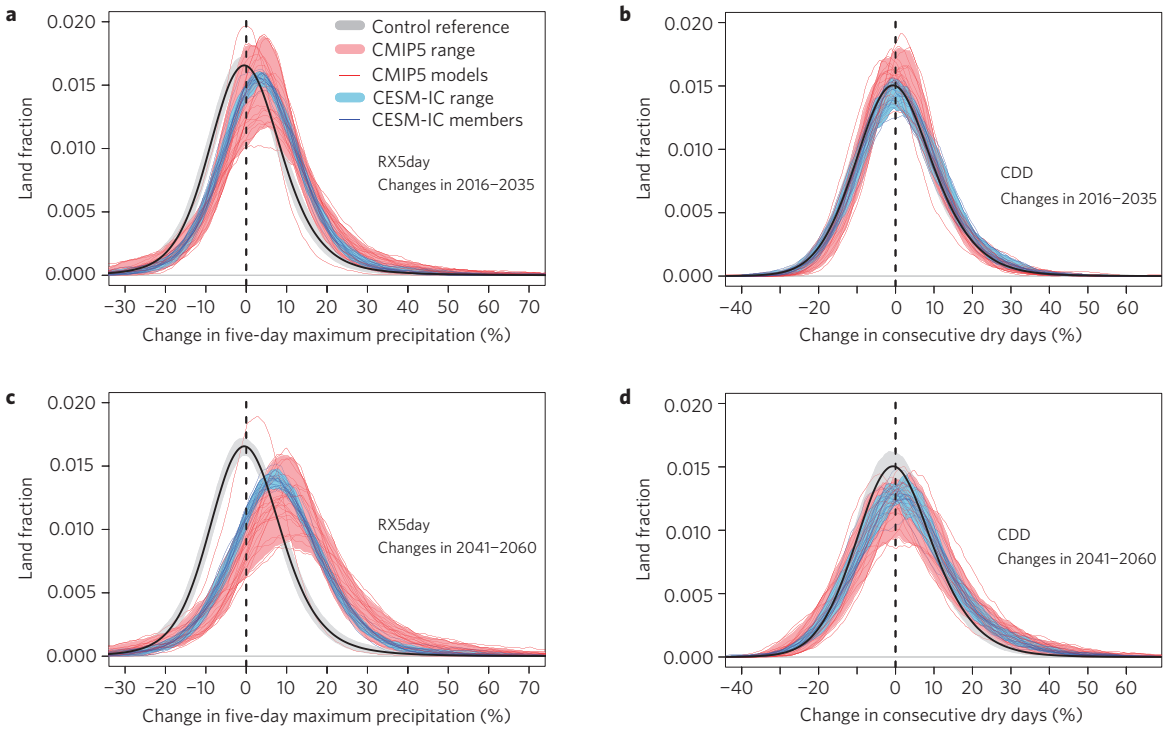

Figure 4 | Spatial distribution of changes in dry spell length and heavy precipitation intensity. a–d, Same as Fig. 3 but for heavy precipitation intensity, RX5day (**a**,**c**) and dry spell length, CDD (**b**,**d**). Legend in **a** applies to all panels. In contrast to Fig. 3 changes at each grid point are expressed as percentages with respect to the climatological mean 1986–2005.

Europe, the US, China and Australia in less than 30 years, and heavy precipitation intensity is projected to increase in those regions over 50 years (Supplementary Figs 11 and 12), thus making the results relevant for decision-makers that are concerned with impacts, cost and adaptation on a national level.

Methods

Model experiment. The simulations are carried out with the CESM version 1.0.4 including the Community Atmosphere Model version 4 (CAM4) and fully coupled ocean, sea ice and land surface components[30]. All simulations are driven with historical forcing until 2005 and RCP8.5 until 2100. On 1 January 1950, a small random perturbation of the order of 10^{-13} is imposed on the atmospheric initial condition field of the reference run to produce a 21-member initial condition ensemble (here referred to as CESM-IC) covering the period 1950–2100. All simulations share the same model version, emission scenario and initial conditions except for the atmosphere. The set-up is very similar to the one described in refs 18,22. After the initial perturbation to the atmospheric initial conditions the model is run freely as a fully coupled Earth system model with no perturbation imposed on any run at any point during the simulation until the end of the run in 2100. Owing to the same ocean initial state the different realizations have similar annual mean temperatures in the first year. However, because of the chaotic nature of the climate system manifesting itself in the internal variability, after a few years the members are in an entirely different state of variability in the ocean, sea ice and atmosphere and thus show a completely different evolution even of global mean temperatures (Supplementary Fig. 2).

Extreme indices. The following standard definition of extreme indices[17] adapted from the Expert Team on Climate Change Detection and Indices for calendar years are used consistent with recent comprehensive analysis of the CMIP5 experiments[12]. All indices are calculated on an annual basis (calendar year):

Intensity of hot extremes (TXx): let TX be the daily maximum temperature, then TXx is the annual maximum value of TX.

Intensity of cold extremes (TNn): let TN be the daily minimum temperature, then TNn is the annual minimum value of TN.

Dry spell length or consecutive dry days (CDD): PR_{ij} is the daily precipitation amount in mm on day i in period j. Count the largest number of consecutive days per time period (here calendar year) where $PR_{ij} < 1$ mm.

Heavy precipitation intensity or maximum accumulated five-day precipitation (RX5day): let PR_k be the precipitation amount in mm for the five-day interval ending on day k. Then RX5day is the annual maximum value of PR_k.

Spatial PDFs. To produce the spatial PDFs in Figs 3 and 4, we calculated changes of 20-year averages of extreme indices at each land grid point (66° N–66° S) between the future and reference period (1986–2005). For temperature extremes (Fig. 3) the local changes are normalized by the standard deviation (in the same model and member, respectively) across the 20 values for the same index in the period 1986–2005. For precipitation extremes the changes are expressed as percentage changes with respect to the local mean of the same model or member in the period 1986–2005. The grid points falling in each bin of the PDF have been weighted according their latitude-dependent area. The PDFs are derived from a rectangular kernel density estimate in statistical package R with only a very weak smoothing applied to retain the information one would see in a histogram. For each member and model the PDFs illustrate the land fraction exhibiting a certain change. The red and blue bands are calculated as 5th to 95th percentile interval for each bin.

Received 19 July 2013; accepted 16 October 2013; published online 17 November 2013

References

1. Donat, M. *et al.* Updated analyses of temperature and precipitation extreme indices since the beginning of the twentieth century: The HadEX2 dataset. *J. Geophys. Res. Atmos.* **118,** 2098–2118 (2013).
2. Meehl, G. A., Tebaldi, C., Walton, G., Easterling, D. & McDaniel, L. Relative increase of record high maximum temperatures compared to record low minimum temperatures in the U. S. *Geophys. Res. Lett.* **36,** L23701 (2009).
3. Perkins, S. E., Alexander, L. V. & Nairn, J. R. Increasing frequency, intensity and duration of observed global heatwaves and warm spells. *Geophys. Res. Lett.* **39,** L20714 (2012).
4. Rahmstorf, S. & Coumou, D. Increase of extreme events in a warming world. *Proc. Natl Acad. Sci. USA* **108,** 17905–17909 (2011).
5. Hansen, J., Sato, M. & Ruedy, R. Perception of climate change. *Proc. Natl Acad. Sci. USA* **109,** E2415–E2423 (2012).
6. Stott, P. A., Stone, D. A. & Allen, M. R. Human contribution to the European heatwave of 2003. *Nature* **432,** 610–614 (2004).
7. Otto, F. E. L., Massey, N., van Oldenborgh, G. J., Jones, R. G. & Allen, M. R. Reconciling two approaches to attribution of the 2010 Russian heat wave. *Geophys. Res. Lett.* **39,** L04702 (2012).
8. Min, S-K., Zhang, X., Zwiers, F. W. & Hegerl, G. C. Human contribution to more-intense precipitation extremes. *Nature* **470,** 378–381 (2011).
9. Trenberth, K. E. Attribution of climate variations and trends to human influences and natural variability. *WIREs Clim. Change* **2,** 925–930 (2011).

© 2013 Macmillan Publishers Limited. All rights reserved.

10. Christidis, N., Stott, P., Brown, S., Hegerl, G. & Caesar, J. Detection of changes in temperature extremes during the second half of the twentieth century. *Geophys. Res. Lett.* **32,** L20716 (2005).
11. Morak, S., Hegerl, G. & Christidis, N. Detectable changes in the frequency of temperature extremes. *J. Clim.* **26,** 1561–1574 (2013).
12. Sillmann, J., Kharin, V., Zwiers, F., Zhang, X. & Bronaugh, D. Climate extremes indices in the CMIP5 multimodel ensemble: Part 2. Future climate projections. *J. Geophys. Res. Atmos.* **118,** 2473–2493 (2013).
13. Tebaldi, C., Hayhoe, K., Arblaster, J. M. & Meehl, G. A. Going to the extremes. *Climatic Change* **79,** 185–211 (2006).
14. Orlowsky, B. & Seneviratne, S. I. Global changes in extreme events: Regional and seasonal dimension. *Climatic Change* **110,** 669–696 (2012).
15. Kharin, V., Zwiers, F., Zhang, X. & Wehner, M. Changes in temperature and precipitation extremes in the CMIP5 ensemble. *Climatic Change* **119,** 345–357 (2013).
16. Seneviratne, S. I. *et al.* in *Managing the Risks of Extreme Events and Disasters to Advance Climate Change Adaptation* (eds Field, C. B. *et al.*) 109–230 (IPCC, Cambridge Univ. Press, 2011).
17. Zhang, X. *et al.* Indices for monitoring changes in extremes based on daily temperature and precipitation data. *WIREs Clim. Change* **2,** 851–870 (2011).
18. Deser, C., Phillips, A., Bourdette, V. & Teng, H. Uncertainty in climate change projections: The role of internal variability. *Clim. Dynam.* **38,** 527–546 (2012).
19. Kenyon, J. & Hegerl, G. Influence of modes of climate variability on global temperature extremes. *J. Clim.* **21,** 3872–3889 (2008).
20. Fischer, E. & Schär, C. Future changes in daily summer temperature variability: driving processes and role for temperature extremes. *Clim. Dynam.* **33,** 917–935 (2009).
21. Hawkins, E. & Sutton, R. The potential to narrow uncertainty in regional climate predictions. *Bull. Am. Meteorol. Soc.* **90,** 1095–1107 (2009).
22. Deser, C., Knutti, R., Solomon, S. & Phillips, A. Communication of the role of natural variability in future North American climate. *Nature Clim. Change* **2,** 775–779 (2012).
23. Kendon, E., Rowell, D., Jones, R. & Buonomo, E. Robustness of future changes in local precipitation extremes. *J. Clim.* **21,** 4280–4297 (2008).
24. Tebaldi, C., Arblaster, J. & Knutti, R. Mapping model agreement on future climate projections. *Geophys. Res. Lett.* **38,** L23701 (2011).
25. Knutti, R. & Sedlacek, J. Robustness and uncertainties in the new CMIP5 climate model projections. *Nature Clim. Change* **3,** 369–373 (2013).
26. Sterl, A. *et al.* When can we expect extremely high surface temperatures? *Geophys. Res. Lett.* **35,** L14703 (2008).
27. Scaife, A., Woollings, T., Knight, J., Martin, G. & Hinton, T. Atmospheric blocking and mean biases in climate models. *J. Clim.* **23,** 6143–6152 (2010).
28. Levy, A. *et al.* Can correcting feature location in simulated mean climate improve agreement on projected changes? *Geophys. Res. Lett.* **40,** 354–358 (2013).
29. Scheff, J. & Frierson, D. Robust future precipitation declines in CMIP5 largely reflect the poleward expansion of model subtropical dry zones. *Geophys. Res. Lett.* **39,** L18704 (2012).
30. Gent, P. *et al.* The community climate system model version 4. *J. Clim.* **24,** 4973–4991 (2011).

Acknowledgements

This research was supported by the Swiss National Science Foundation.

Author contributions

E.M.F. carried out the analysis of the models, U.B. carried out the model experiment. All authors contributed extensively to the idea and the writing of this paper.

Additional information

Supplementary information is available in the online version of the paper. Reprints and permissions information is available online at www.nature.com/reprints. Correspondence and requests for materials should be addressed to E.M.F.

Competing financial interests

The authors declare no competing financial interests.

© 2013 Macmillan Publishers Limited. All rights reserved.